



Title:

Statistical Shape Modeling for Virtual Femur Reconstruction: An Innovative Approach to Allograft Selection

Authors:

Alessio Romanelli, alessio.romanelli@unifi.it, University of Florence
Michaela Servi, michaela.servi@unifi.it, University of Florence
Maurizio Scorianz, scorianzm@aou-careggi.toscana.it, AOU Careggi
Domenico Andrea Campanacci, campanaccid@aou-careggi.toscana.it, AOU Careggi
Yary Volpe, yary.volpe@unifi.it, University of Florence

Keywords:

CAD, Surgical Planning, Statistical Shape Model, Orthopedics, Reconstruction

DOI: 10.14733/cadconfP.2025.38-43

Introduction:

The treatment of malignant bone tumors of the knee often requires the removal of the diseased femur/tibia affected segment using planned cutting planes, followed by the implant of a prosthesis [2]. Another widely used approach involves reconstruction using an allograft, which is bone tissue harvested from a donor [5]. Donor bones are typically supplied by musculoskeletal tissue banks, facilities dedicated to harvesting, preserving, and distributing tissues for transplantation.

Selecting the most appropriate donor is a complex process, where matching the size and shape of the recipient bone plays a vital role in providing good integration. A closer shape matching between donor and recipient can also improve post-operative outcomes, lowering the possibility of fractures or non-unions [13]. Furthermore, allografts taken from the same anatomical site as the affected area exhibit similar mechanical and osteoconductive properties [16]. However, the tumor often alters the recipient bone structure, making it difficult to compare directly with the potential donor bones.

To overcome this challenge, virtual reconstruction of premorbid anatomy is a common approach. The contralateral method, considered the gold standard, consists in the creation of a mirrored 3D model of the healthy contralateral bone, providing an accurate representation of the premorbid anatomy of the affected bone. [4, 6, 15].

Nevertheless, this approach is not always a viable option since it requires CT scans of both limbs. Many times, this is not possible since this would expose the patient to an excessive dose of x-ray, and, anyway, it still requires the contralateral to be healthy, which sometimes may not be the case. Another widely used tool for anatomy reconstruction is Statistical Shape Model (SSM). SSM can learn shape variation from a class of given samples and represent the shape variation using the leading principal components. SSM has been used for reconstruction of the premorbid anatomy of a variety of different bones in the context of many surgical procedures [8, 14, 17].

However, as far as it is known, SSM has never been used for anatomy reconstruction in the context of allograft selection. Therefore, the aim of this work is to develop and evaluate the ability of an SSM to reconstruct the full anatomy of the femur in order to provide a reliable reconstruction that can be used as a comparison to possible donor bones thus improving the allograft selection process.

Statistical Shape Model Definition:

The main assumption of a Statistical Shape Model is that all possible shape deformations can be learned from a set of M samples forming an appropriate Training Set $\{\Gamma^1, \Gamma^2, \dots, \Gamma^M\}$. A complex shape Γ^i can be described as a dense set of landmarks x_k distributed on the surface:

$$\Gamma^i = \{x_k^i \mid x_k^i \in \mathbb{R}^3, k = 1, \dots, N_i\}$$

where N_i is the number of points used to describe the shape i , and x_k contains the 3 Cartesian coordinates of the k -th point.

The crucial assumption is that the landmark points are in correspondence among the samples. This means that the k -th landmark of two shapes Γ^i and Γ^j represents the same anatomical point of the shape. Finding a meaningful correspondence between shapes is one of the critical tasks of statistical shape analysis. Once it is established, all shapes can be described with the same number of points N . Therefore, by defining each shape Γ^i as a vector $\vec{x}_i \in \mathbb{R}^{3N}$ consisting of the stacked x, y, z components of each point, the shape variations can be modeled using a normal distribution, where the mean \bar{x} and covariance matrix L are estimated as follows:

$$\bar{x} = \frac{1}{M} \sum_{i=1}^M \vec{x}_i \quad (1)$$

$$L = \frac{1}{M-1} \sum_{i=1}^M (\vec{x}_i - \bar{x})(\vec{x}_i - \bar{x})^T \quad (2)$$

However, since the number of landmark points describing the samples is usually quite large, a high amount of data is necessary to represent the covariance matrix L explicitly. Fortunately, as it is determined completely by the M samples, it has at most rank M and can therefore be represented using M basis vectors. This is achieved by performing a Principal Component Analysis [7], thus leading to the following definition of SSM:

$$x = \bar{x} + \sum_{m=1}^c \alpha_m \sqrt{\lambda_m} \varphi_m \quad (3)$$

Where λ_m and φ_m are, respectively, the eigenvalues and eigenvectors of matrix L , α_m follows a normal distribution with mean = 0 and sigma = 1 and c represents the number of significant eigenvalues. The number c is defined so that the accumulated variance reaches a certain ratio of the total variance, usually between 0.9 and 0.98 (in this work 0.98 is used). Equation 3 allows to have an efficient, parametric representation of the distribution.

Although the entire process appears simple, determining the correspondences is a challenging step since the quality of the SSM itself is heavily influenced by the established correspondences. The most widely used methods for this task rely on the Iterative Closest Point (ICP) algorithm [1] or the Coherent Point Drift (CPD) algorithm [11]. In this work the algorithm described in [9] is used to establish correspondences between samples of the training set.

For this study, the training set consisted of 78 healthy right femurs (42 males, 36 females, mean age: 29.4 years). The 3D models of the femurs were obtained by segmentation, using the software Materialise Mimics 26 [10], of post-mortem Computed Tomography Images obtained from the New Mexico Decedent Image Database [3]. In order to reduce computational load 3D models were then decimated to 20000 points. The 3D models were first translated to align their centroid with the origin of the Global Reference System. After that a reference shape was chosen randomly from the training set and all other femurs were aligned to the reference using rigid ICP algorithm in order to remove relative rotation between the models. Then the algorithm described in [9] was used to establish correspondences. At this point the mean shape and the covariance matrix could then be computed

through Equation 1 and 2. By performing Principal Component Analysis, the SSM was defined through Equation 3.

Statistical Shape Model Evaluation:

The most widely used approach for assessing the quality of an SSM is based on three key properties: Generalization, Specificity, and Compactness [8].

The first property, Generalization (G), measures how well the SSM can replicate a given shape. It is typically assessed through a series of leave-one-out tests on the training set, by computing the distance between the omitted shape Γ^i and its closest match $\Gamma_*^i(c)$ generated by the reduced SSM. The Generalization is given as a function of the number c of the significant eigenvalues used to define the parametric model:

$$G(c) = \frac{1}{M} \sum_{i=1}^M D(\Gamma_*^i(c), \Gamma^i) \quad (4)$$

Lower G values correspond to better-performing SSMs. The metric D is used to quantify the distance between shapes. Following the approach in [8], this study uses the Symmetric Mean (SM) distance as metric D .

The second metric is Specificity (S), which evaluates the ability of the model to produce new shapes that are consistent with the family of shapes encoded in the model. This is evaluated by generating random parameter sets of α and calculating the average distance between each corresponding generated shape $\Gamma_{**}^k(c)$ and its nearest match in the training set, over a large number of iterations (t). As a Generalization, Specificity is given as a function of the number of significant eigenvalues c :

$$S(c) = \frac{1}{t} \sum_{k=1}^t \min_{i=1, \dots, M} D(\Gamma_{**}^k(c), \Gamma^i) \quad (5)$$

where the metric D used for Specificity is the Mean Absolute Distance between corresponding points to make the measurement robust and independent from the number of landmarks [8].

Interestingly, $S(c)$ tends to worsen as c increases. While this may seem counterintuitive, it can be explained by noticing that greater variability allows the SSM to elude the training set members more easily.

The last metric, Compactness (C), represents the cumulative variance of the model as determined by principal component analysis (PCA). In this work C was normalized with respect to the total variance:

$$C(c) = \frac{\sum_{i=1}^c \lambda_i}{\sum_{j=1}^{M-1} \lambda_j} \quad (6)$$

A compact model, characterized by a low c value, requires fewer parameters to encode greater variability within the training set. In contrast to the first two measures, higher C values correspond to better SSMs.

Generalization, Specificity, and Compactness for the SSM constructed in this work are reported in Fig. 1. As can be seen from Fig. 1c the first mode of variation accounts for 90.7 % of the total variance of the model. Compactness grows quickly reaching the value of 98% for $c = 13$, indicating that a compact model can represent the great majority of the possible shapes encoded in the model. Furthermore from Fig. 1a-b it can be noted how the curves of Generalization and Specificity flatten for $c > 10$ meaning that $c = 13$ is a good choice to balance the ability to replicate a given shape

($G = 0.990$ mm for $c = 13$) and the ability to generate new shapes consistent with the family of shapes encoded in the model ($S = 4.622$ mm for $c = 13$).

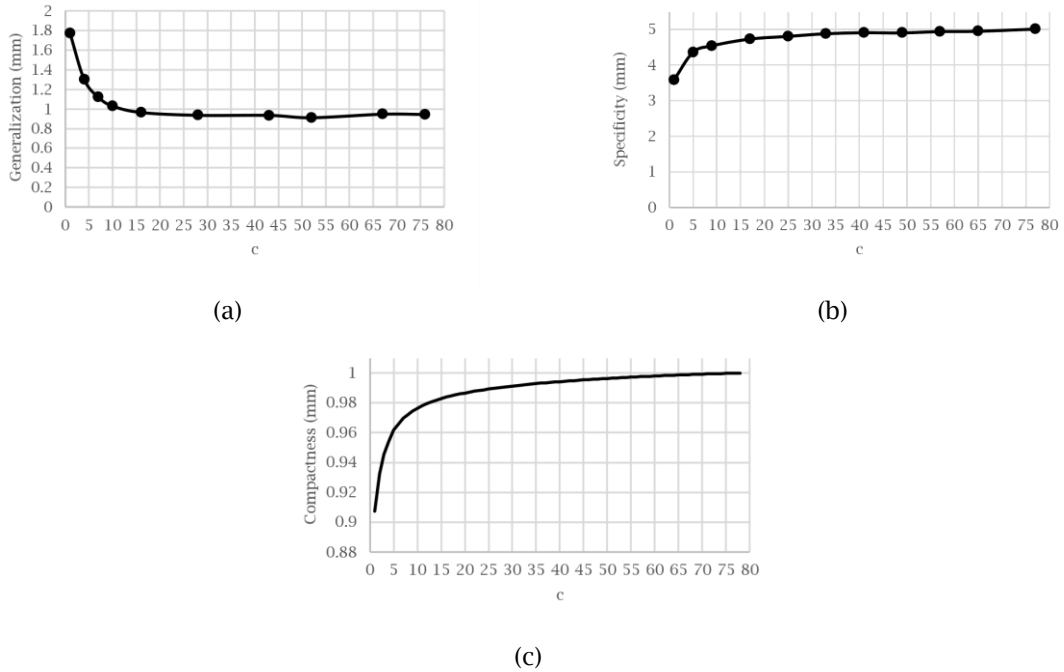


Fig. 1: (a) Generalization, (b) Specificity, (c) Compactness as a function of modes of variation c .

Reconstruction of missing anatomy:

After building and evaluating the SSM, its ability to infer the complete shape of a femur from a partial one was tested. A dataset of 49 femurs was chosen randomly from the 78 femurs composing the training set of the SSM.

Through the software Geomagic Design X [12], 20 different configurations of resection were generated and replicated on each of the 49 cases in the dataset such that a total of 980 partial femurs representing simulated clinical cases, were obtained.

A series of leave-one-out tests were performed meaning that for each of the 49 cases, an SSM was built using the remaining 77 femurs, then the reduced SSM was used to infer the full shape of the femur for the 20 different resections using $c = 13$. Three examples of reconstruction are reported in Fig. 2.

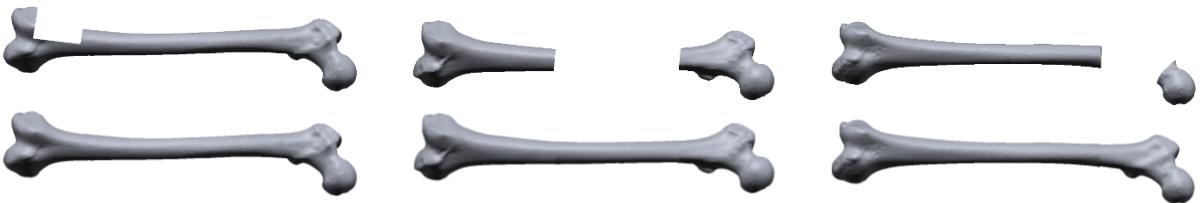


Fig. 2: Examples of reconstruction using 13 modes of variation.

To evaluate the similarity between the reconstructions generated by the SSM and the real anatomy of the bone, Chamfer Distance (CD) and Hausdorff Distance (HD) were used. CD and HD between two-point clouds P_1 and P_2 can be defined as:

$$CD_{P_1, P_2} = \frac{1}{2} \left(\frac{1}{|P_1|} \sum_{x \in P_1} \|x - \bar{y}\|_2 + \frac{1}{|P_2|} \sum_{y \in P_2} \|y - \bar{x}\|_2 \right) \quad (7)$$

$$HD_{P_1, P_2} = \frac{1}{2} \left(\max_{x \in P_1} \|x - \bar{y}\|_2 + \max_{y \in P_2} \|y - \bar{x}\|_2 \right) \quad (8)$$

where $\bar{y} = \left\{ y \in P_2 \mid d(x, y) = \min_{y \in P_2} \|x - y\|_2 \right\}$ (and similarly for \bar{x}) while $|P_1|$ and $|P_2|$ represent the number of points of each point cloud. Thus CD can be intended as the mean distance between the two point clouds, while the HD as the maximum distance. In

Fig. 3 the mean and standard deviation of HD and CD , calculated across all 980 cases, are reported. As can be seen, the constructed SSM was able to reconstruct the missing anatomy with a mean CD of 1.066 mm.

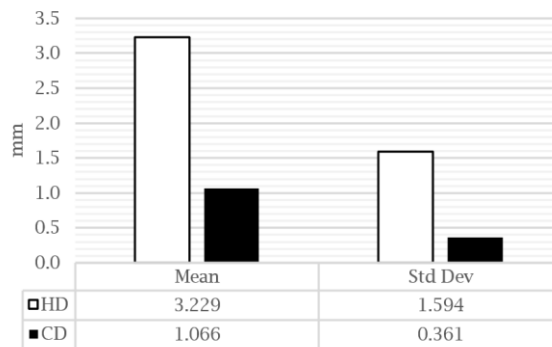


Fig. 3: Chamfer Distance and Hausdorff Distance mean and standard deviation across all 980 reconstructions.

Acknowledgements:

The authors wish to acknowledge the Tuscany Region (Italy) for co-funding the PRECISE project (BANDO RICERCA SALUTE 2018), which originated and made this research possible.

Alessio Romanelli, <https://orcid.org/0009-0009-2941-6740>

Michaela Servi, <https://orcid.org/0000-0002-4071-6615>

Maurizio Scorianz, <https://orcid.org/0000-0002-7164-065>

Yary Volpe, <https://orcid.org/0000-0002-5668-1912>

References:

- [1] Besl, P.-J; McKay, N.-D: A Method for Registration of 3-D Shapes, IEEE Transactions on Pattern Analysis and Machine Intelligence, 14(2), 1992, 239-256. <https://doi.org/10.1109/34.121791>
- [2] Calderón, S.-A.-L.; Kuechle, J.; Raskin, K.-A., Hornicek, F.-J.: Lower Extremity Megaprotheses in Orthopaedic Oncology, The Journal of the American Academy Orthopaedic Surgeons, 26(12), 2018 e249-e257. <https://doi.org/10.5435/JAAOS-D-16-00218>
- [3] Edgar, H.-J.-H.; Daneshvari, Berry S.; Moes, E.; Adolphi, N.; Bridges, P.; Nolte, K.: New Mexico Decedent Image Database, Office of the Medical Investigator, University of New Mexico, 2020.

- [4] Ferràs-Tarragó, J.; Sanchis-Alfonso, V.; Ramírez-Fuentes, C.; Roselló-Añón, A.; Baixauli-García, F.: A 3D-CT Analysis of Femoral Symmetry—Surgical Implications, *Journal of Clinical Medicine* 9(11), 2020, 3546. <https://doi.org/10.3390/jcm9113546>
- [5] Houdek, M.-T.; Sullivan, M.-H.; Broida, S.-E.; Barlow, J.-D.; Morrey, M.-E.; Moran, S.-L.; Sanchez-Sotelo, J.: Proximal Humerus Reconstruction for Bone Sarcomas: A Critical Analysis, *JBJS Reviews*, 12(3), 2024. <https://doi.org/10.2106/IBJS.RVW.23.00217>
- [6] Jacquet, C.; Laumonerie, P.; LiArno, S.; Faizan, A.; Sharma, A.; Dagneaux, L.; Ollivier, M.: Contralateral preoperative templating of lower limbs' mechanical angles is a reasonable option, *Knee Surgery, Sports Traumatology, Arthroscopy*, 28(5), 2020, 1445-1451. <https://doi.org/10.1007/s00167-019-05524-0>
- [7] Jolliffe, I.-T.: *Principal Component Analysis*, Springer New York, New York, NY, 2002. <https://doi.org/10.1007/b98835>
- [8] Marzola, A.; McGreevy, K.-S.; Mussa, F.; Volpe, Y.; Governi, L.: HyM3D: A hybrid method for the automatic 3D reconstruction of a defective cranial vault, *Computer Methods and Programs in Biomedicine*, 2023, 234. <https://doi.org/10.1016/j.cmpb.2023.107516>
- [9] Marzola, A.; Servi, M.; Volpe, Y.: A Reliable Procedure for the Construction of a Statistical Shape Model of the Cranial Vault, *Lecture Notes in Mechanical Engineering*, 2020, 788-800. https://doi.org/10.1007/978-3-030-31154-4_67
- [10] Materialise Mimics 26, <https://www.materialise.com/en/healthcare/mimics-innovation-suite/26>, Materialise, 2023.
- [11] Myronenko, A.; Song, X.: Point set registration: coherent point drift, *IEEE Transactions on pattern analysis machine intelligence*, 2010, 32(10), 2262-2275. <https://doi.org/10.1109/TPAMI.2010.46>
- [12] Geomagic Design X 2024.1, <https://oqton.com/geomagic-designx>, Oqton, 2024.
- [13] Pala, E.; Canapeti, J.; Trovarelli, G.; Angelini, A.; Ruggieri, P.: Is still effective massive allograft reconstruction in parosteal osteosarcoma of the distal femur? Review of the literature and advantages of newer technologies, *Journal of Orthopaedic Surgery and Research*, 2024, 19(1), 395. <https://doi.org/10.1186/s13018-024-04880-z>
- [14] Salhi, A.; Burdin, V.; Boutillon, A.; Brochard, S.; Mutsvangwa, T.; Borotikar, B.: Statistical Shape Modeling Approach to Predict Missing Scapular Bone, *Annals of Biomedical Engineering*, 2020, 48(1), 367-379. <https://doi.org/10.1007/s10439-019-02354-6>
- [15] Sparks, C.-A.; Decker, S.-J.; Ford J.-M.: Three-Dimensional Morphological Analysis of Sex, Age, and Symmetry of Proximal Femurs from Computed Tomography: Application to Total Hip Arthroplasty, *Clinical Anatomy*, 2020, 33(5), 731-738. <https://doi.org/10.1002/ca.23496>
- [16] Wu, Z.; Fu, J.; Wang, Z.; Li, X.; Li, J.; Pei, Y.; Pei, G.; Li, D.; Guo, Z.; Fan, H.: Three-dimensional virtual bone bank system for selecting massive bone allograft in orthopaedic oncology, *International Orthopaedics*, 2015, 39(6), 1151-1158. <https://doi.org/10.1007/s00264-015-2719-5>
- [17] Zhou, C.; Cha, T.; Peng, Y.; Bedair, H.; Li, G.: 3D Geometric Shape Reconstruction for Revision TKA and UKA Knees Using Gaussian Process Regression *Annals of Biomedical Engineering*, 2021, 49(12), 3685-3697. <https://doi.org/10.1007/s10439-021-02871-3>